Materials Research Letters ›
Volume 4, 2016 - Issue 3

Original Reports

Back stress strengthening and strain hardening in gradient structure

Muxin Yang, Yue Pan, Fuping Yuan, Yuntian Zhu & Xiaolei Wu

Pages 145-151 | Received 14 Jan 2016, Accepted 08 Feb 2016, Published online: 02 Mar 2016

Cite this article https://doi.org/10.1080/21663831.2016.1153004 Check for updates

Abstra

We repo ... dient
structure ... used by the
pileup o ... nd a
procedu ... hysics from
the tens ... mechanical
incor ... which needs
to be ... h but also
significa

Impact S ... o increase
strength ... e back
stress fr

GRAPHICAL ABSTRACT

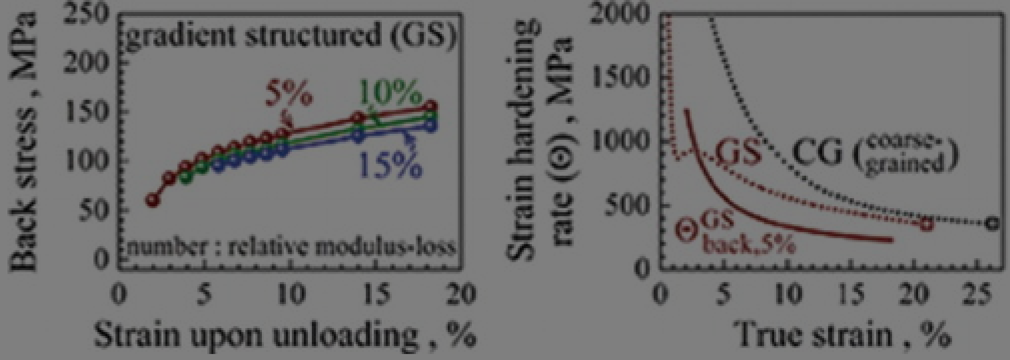

Keywords:

Back Stress · Geometrically Necessary Dislocations · Work Hardening · Ductility · Gradient Structure

Gradient structure in metals represents a new strategy for producing a superior combination of high strength and good ductility.[1–6] The gradient structure usually consists of a nanostructured (NS) surface layer with increasing grain size along the depth to reach coarse-grained (CG) sizes in the central layer.[2,4]

Gradient structure can promote ductility significantly,[2,4–9] which is measured under tensile loading. The NS layer in a gradient structure may sustain a large amount of

tensile s orted that
the grad f the soft CG
core,[2,1 iven grain
growth c known to
be unsta
nanocry s with stable
gradient hardening
due t h generates
geon and
interacti s observed
to produ ch higher
than tha] which is
attribute tween
layers.[3

The nature of plastic deformation in the gradient structure is still not very clear.[1,2] In fact, the gradient structure can be approximately regarded as the integration of many thin layers with increasing grain sizes.[3,4] The gradient structure deforms heterogeneously due to plastic incompatibilities between neighboring layers with different flow behaviors and stresses under applied strains. As such, it is reasonable to anticipate the development of the strain gradient and internal stresses during plastic deformation, as a result of the plastic incompatibilities between different layers, similar to what happens in composites [19–21] and dual-phase structures.[22]

Back stress has been reported to play a crucial role in strain hardening, strengthening and mechanical properties.[21–23] It is a type of long-range stress exerted by GNDs that are accumulated and piled up against barriers. It interacts with mobile dislocations to affect their slip.[24] The back stress reduces the effective resolved shear stress for dislocation slip because it always acts in the opposite direction of the applied resolved shear stress. In a heterogeneous structure, strain will be inhomogeneous but continuous, producing strain gradients, which needs to be accommodated by GNDs. [23,25–27] It has been observed that back stress strengthening and back stress strain-hardening are primarily responsible for unprecedented combination of strength and ductility of heterogeneous lamella Ti, which was found as strong as ultrafine-grained Ti and as ductile as CG Ti.[23] The gradient structure can be regarded as a type of
heteroge ... ant back
stress w ... to have a
better u

Here we ... gnificant
back str ... ound physics
to calcul ... s loop
during a ... m the
hyst

A 1-mm ... terials with
the com ... P, 0.037% Al,
0.063% ... ealed at
1173 K f ... grain size of
35 μm. S ... duce the GS
sample. ... er of 120
μm thick was formed, which consists of, in sequence, the nanograins (minimum grain

size of <100 nm in the top layer), ultrafine grains, and deformed coarse grains with dislocation cells towards the central CG core. Microstructural characterization was detailed in our previous papers.[3,4]

Unloading–reloading process during tensile tests was conducted using an Instron 5966 machine at a strain rate of $5 \times 10^{-4}\,s^{-1}$ at room temperature. Tensile specimens with a gauge length of 10 mm and a width of 2.5 mm were cut from SMAT-processed disks. An extensometer was used to measure tensile strain. At a certain unloading strain, the specimen was unloaded in a load-control mode to 20 N at an unloading rate of 200 N min^{-1}, followed by reloading to the same applied load.

Figure 1(a) shows the monotonic tensile true stress–true strain (σ–) curves in both GS and CG samples. The GS sample shows large tensile ductility comparable to that of CG, but with triple yield strength of CG, which is typical of the excellent combination of strength and ductility in GS metals.[2–8] A transient is visible soon after yielding, characterized by the presence of a short concave segment on the σ– curve.[4] During the transient, the strain hardening rate (Θ) sharply drops at first, which is followed by a rapid up-turn, as shown in Figure 1(b). Figure 1(c) shows the unloading and reloading test hysteresis loops measured at varying tensile strains for both CG and GS samples.

Figure 1. (Colour online) (a) Tensile stress–strain curves in the GS and CG IF steel samples … nd reloading test hyst … S samples.

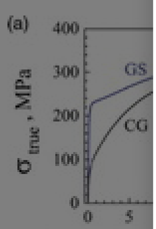

Display

Unloadir … the
evolutio … the
unloadir … starts at
unloadir … uasi-elastic
and cau … The stress
drop in t … ,29] or
viscous … oading stress

with an effective unloading Young's modulus of E_u. The point C is called the unloading yielding point, with a stress of σ_u. Similar segments also exist for the reloading curve with EF as the linear (elastic) part of the reloading stress–strain curve with an effective reloading Young's modulus of E_r, which can be assumed equal to E_u because the microstructure is assumed not changed during the unloading–reloading. The point F is called the reloading yielding point, with a stress of σ_r. Figure 2(b) is the measured hysteresis loop from a GS IF steel sample.

Figure 2. (Colour online) (a) The schematic of the unloading–reloading loop for defining the unload yielding σ_u, reload yielding σ_r, back stress σ_b and frictional stress σ_f, effective unloading Young's modulus of E_u, effective reloading Young's modulus of E_r. (b) A measured hysteresis loop from the GS IF steel sample with σ_u and σ_r defined.

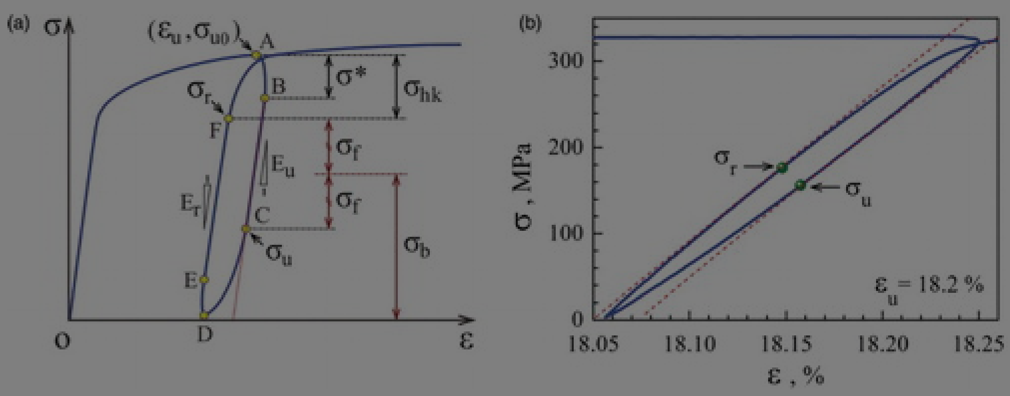

Display full size

From the ... ress σ_b, and
the fricti ... the applied
stress, w ... ion of
dislocati ... er stresses
that are ... olute atoms,
second

To de ... ve first
assum ... –reloading
process. ... ng before
the unlo ... cause the
reverse ... NDs that
produce ... the
unloadir ... ssumption
is impor ... ng, the back
stress is the stress that drives the mobile dislocations to reverse their gliding direction

to produce unloading yield. At the unloading yield point C (Figure 2(a)), the applied stress is low enough that the back stress starts to overcome the applied stress and the frictional stress to make dislocations glide backward, that is

(1)

where σ_u is the unloading yield stress as defined in Figure 2(a).

During the reloading, the applied stress needs to overcome the back stress and the frictional stress to drive the dislocation forward at the reloading yield point F, which can be described as

(2)

where σ_r is the reloading yield stress as defined in Figure 2(a).

Here again, we assume that the back stress during reloading is the same as the back stress during unloading. This is reasonable because during the unloading–reloading process, dislocation configuration can be considered reversible.[32] Solving Equations (1) and (2) yields

(3)

and

(4)

Equation (3) is similar to an earlier equation proposed for cyclic loading by Cottrell [33] and Kulm tress at the

beginnir

where σ

We argu we are

defining s, the same

deviatio nized that

Equati son et al. to

inclu

where σ (a),[24,29]

which is

Equatior ng yield

stresses come

negative we expect

Equation (3) to be valid if the applied stress is reversed to negative to measure σ_u

before the reloading. As discussed later, Equation (3) derived here has an important advantage over previously published Equations (5) and (6): it produces consistent back stress values with much less scatter. In addition, Equations (5) and (6) are physically problematic because they implicitly used different criteria to define the unloading yield and reloading yield, which is physically unjustifiable.

To extract useful data from the unloading–reloading hysteresis loop, one needs to first determine the unloading yield stress σ_u and reloading yield stress σ_r. However, the real hysteresis loop (e.g. Figure 2(b)) is not as well defined as in Figure 2(a), and the practical extraction of the data is not straightforward.[31] The first step is to determine the elastic segments BC as well as its slope (the effective Young's modulus). The unloading yield point C is usually determined by a plastic strain offset in the range of 5×10^{-6} to 10^{-3}, which have been used by different research groups.[24,31,34–37] These offset values are arbitrary and are not well justified. Here we propose to use the deviation of the stress–strain slope from the effective Young's modulus as a physically sound method to determine the yield point. In this study, we choose 5%, 10%, and 15% slope reduction from the effective Young's modulus, E_u. If the strain hardening in the plastically deforming volume is ignored, the slope reduction should be equal to the volume fraction that is plastically deforming. For example, a 10% reduction in E_u means 10% of the sample volume is plastically deforming. We also propose to use $E_r = E_u$, and the sam … oint and reloadin …

Figure 3 … ld stress, and bac … train at which th … gure. First, the unlo … y the slope reductio … . Second, using … higher reloadi … choice of slope re … atter in the calculate … vantage of Equatior … y reported Equatior … samples increase … S sample than in t … tress in the GS sample is 10–40% higher than those in the CG sample (the red curves in Figure 3(b) and 3(d)). Fourth, Figure 3(c) and 3(d) shows that if a large slope reduction value is used, the unloading yield stresses for the GS sample at small tensile strains are negative and therefore cannot be measured in the unloading curve. This makes it advantageous to use a smaller slope reduction value in determining the back stress.

Figure 3. (Colour online) Evolution of (a) unloading yield stress σ_u and reloading yield stress σ_r and (b) back stress with increasing unloading strain $_u$ for CG IF steel, and the evolution of (c) unloading/reloading yield stresses and (d) back stress with increasing $_u$ for GS IF steel. $\sigma_{b,5\%}$ represents the back stress calculated using 5% slope reduction from the effective Young's modulus.

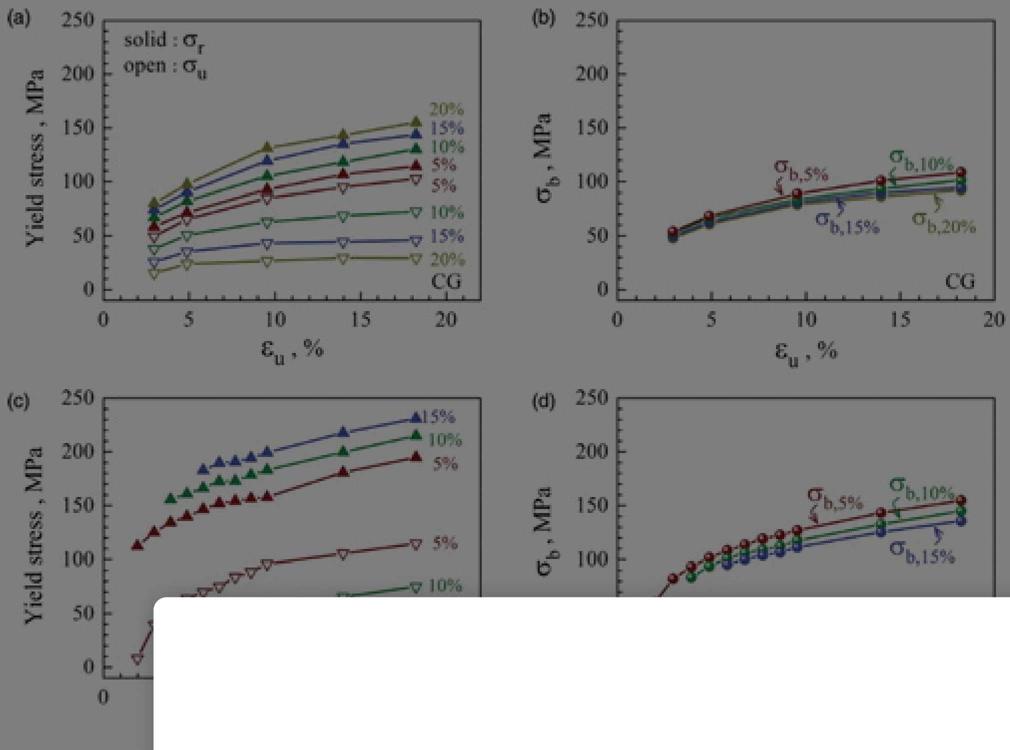

Display ful

For valid ... or
calculati ... resents back
stress ca ... lus, as
show ... g E_u, E_r, and
the corre ... e linear
parts of ... of these
uncertai

As show ...) is very
scattere ... example,
for the C ... es larger
than those calculated using the 5% slope reduction. This is because Equation (4) adds

the absolute values of σ_u and σ_r variations together instead of making them cancel each other as in Equation (3). Therefore, the frictional stress σ_f calculated using Equation (4) is not quantitatively dependable. Nevertheless, Figure 4(a) consistently shows that for any slope reduction value, the calculated frictional stress is higher in the GS sample than in the CG sample. This is due to the higher dislocation density in the GS sample than in the CG sample.[3,4]

Figure 4. (Colour online) The frictional stress σ_f vs. tensile strain $_{true}$ for the GS and CG IF steel samples calculated according to Equation (4). (b) The distinct back stress hardening in GS IF steel. denotes the back stress hardening rate calculated using 5% slope reduction from the effective Young's modulus.

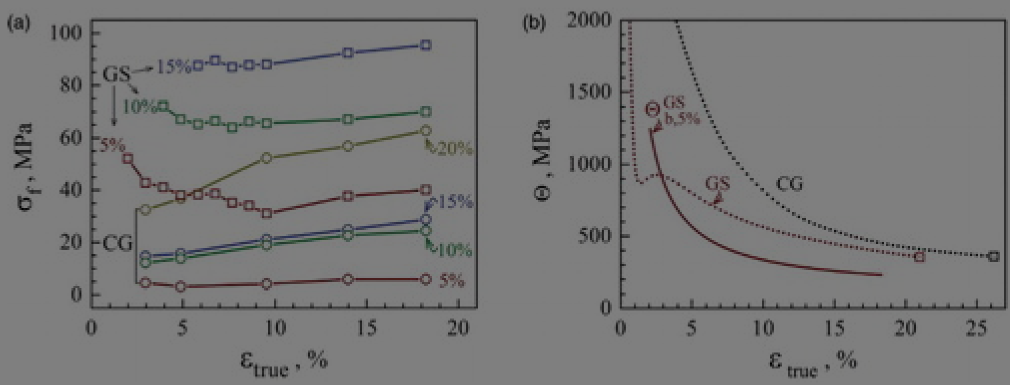

Display full size

Figure 4 ardening

than the the

transien ess strain-

hardenir back stress

increase (d). The

observe e to the

back str ns.[4] The

high b gests that a

large sociated

with the here was a

quick in tion of the

GS IF ste in which

the NS s endicular to

the tens ally, the

surface stress, while

the central larger grained layer transits in an opposite way. Such a transition is expected to increase the strain gradient.

In summary, it is found that the GS IF steel developed strong back stress strengthening and back stress strain-hardening during tensile testing, which arise from the plastic incompatibilities due to its microstructural heterogeneity. The high back stress near the beginning of the plastic deformation of the GS IF steel samples should have contributed to the observed synergetic strengthening,[3] while the high back stress hardening should have contributed to the observed high ductility.[4] The equation derived and the procedure proposed in this work for calculating the back stress from the unloading–reloading hysteresis loop produces more consistent back stress value than what is previously reported.

Acknowledgements

This work was supported by the National Natural Science Foundation of China under Grant numbers (11572328, 11072243, 11222224, 11472286, and 51471039); and 973 Projects under Grant numbers (2012CB932203, 2012CB937500, and 6138504). Y.T.Z. is funded by the US Army Research Office (W911 NF-12–1–0009), the US National Science Foundati

Micro&N

Disclo

No poter

Refer

1. Lu K. I

2014;

2. Fang TH, Li WL, Tao NR, Lu K. Revealing extraordinary intrinsic tensile plasticity in gradient nano-grained copper. Science. 2011;331(6024):1587–1590. doi: 10.1126/science.1200177

PubMed | Web of Science ® | Google Scholar

3. Wu XL, JIang P, Chen L, et al. Synergetic strengthening by gradient structure. Mater Res Lett. 2014;2(4):185–191. doi: 10.1080/21663831.2014.935821

Web of Science ® | Google Scholar

4. Wu XL, Jiang P, Chen L, Yuan FP, Zhu YT. Extraordinary strain hardening by gradient structure. Proc Natl Acad Sci USA. 2014;111(20):7197–7201. doi: 10.1073/pnas.1324069111

PubMed | Web of Science ® | Google Scholar

5. Jerusalem A, Dickson W, Perez-Martin MJ, Dao M, Lu J, Galvez F, Grain size gradient length scale in ballistic properties optimization of functionally graded nanocrystalline steel plates. Scr Mater. 2013;69(11):773–776. doi: 10.1016/j.scriptamat.2013.08.025

Web of Science ® | Google Scholar

6. Wang … winned
structu…
10.10…

7. Ko… …orphous
me…
10.10…

8. Wei YJ … …ma in steel
throug… …580.

PubMed | Web of Science ® | Google Scholar

9. Ma XL, Huang CX, Xu WZ, Zhou H, Wu XL, Zhu YT. Strain hardening and ductility in a coarse-grain/nanostructure laminate material. Scr Mater. 2015;103:57–60. doi: 10.1016/j.scriptamat.2015.03.006

Web of Science ® | Google Scholar

10. Fang TH, Tao NR, Lu K. Tension-induced softening and hardening in gradient nanograined surface layer in copper. Scr Mater. 2014;77:17–20. doi: 10.1016/j.scriptamat.2014.01.006

Web of Science ® | Google Scholar

11. Weertman JR. Retaining the nano in nanocrystalline alloys. Science. 2012;337(6097):921–922. doi: 10.1126/science.1226724

PubMed | Web of Science ® | Google Scholar

12. Chookajorn T, Murdoch HA, Schuh CA. Design of stable nanocrystalline alloys. Science. 2012;337(6097):951–954. doi: 10.1126/science.1224737

PubMed | Web of Science ® | Google Scholar

13. Zhang ... in
nanoc ... tt.
2005;

14. Zhang ... and grain
siz ... n copper.
Ap

15. Legros ... oundary
motio ... 14):3380–
3393.

Web of Science ® | Google Scholar

16. Liao XZ, Kilmametov AR, Valiev RZ, Gao HS, Li XD, Mukherjee AK, Bingert JF, Zhu YT. High-pressure torsion-induced grain growth in electrodeposited nanocrystalline Ni. Appl Phys Lett. 2006;88: Article no. 021909. doi: 10.1063/1.2159088

Web of Science ® | Google Scholar

17. Li WB, Yuan FP, Wu XL. Atomistic tensile deformation mechanisms of Fe with gradient nano-grained structure. AIP Advances. 2015;5(8): Article no. 087120. doi: 10.1063/1.4928448

Google Scholar

18. Li JJ, Chen SH, Wu XL, Soh AK. A physical model revealing strong strain hardening in nano-grained metals induced by grain size gradient structure. Mater Sci Eng A. 2015;620:16–21. doi: 10.1016/j.msea.2014.09.117

Web of Science ® | Google Scholar

19. Llorca J, Needleman A, Suresh S. The Bauschinger effect in whisker-reinforced metal-matrix composites. Scr Metall Mater. 1990;24(7):1203–1208. doi: 10.1016/0956-716X(90)90328-E

20. Sincla … two-phase
mater …
10.10 …

21. Th … n
Swyge … rials:
applic … Acta Mater.
2009; …

22. Calcagnotto M, Adachi Y, Ponge D, Raabe D. Deformation and fracture mechanisms in fine- and ultrafine-grained ferrite/martensite dual-phase steels and the effect of aging. Acta Mater. 2011;59:658–670. doi: 10.1016/j.actamat.2010.10.002

Web of Science ® | Google Scholar

23. Wu XL, Yang MX, Yuan FP, Wu GL, Wei YJ, Huang XX, Zhu YT. Heterogeneous lamella structure unites ultrafine-grain strength with coarse-grain ductility. Proc Natl Acad Sci USA. 2015;112(47):14501–14505. doi: 10.1073/pnas.1517193112

PubMed | Web of Science ® | Google Scholar

24. Feaugas X. On the origin of the tensile flow stress in the stainless steel AISI 316L at 300 K: back stress and effective stress. Acta Mater. 1999;47(13):3617–3632. doi: 10.1016/S1359-6454(99)00222-0

Web of Science ® | Google Scholar

25. Ashby MF. The deformation of plastically non-homogeneous materials. Philos Mag. 1970;21(170):399–424. doi: 10.1080/14786437008238426

Web of Science ® | Google Scholar

26. Gao H ... nt plasticity - I Theo ... 5096(...

27. Ga ... ent plasticity. Sc ...

28. Lu K, L ... surface mecha ... oi: 10.10 ...

Web of Science ® | Google Scholar

29. Dickson JI, Boutin J, Handfield L. A comparison of two simple methods for measuring cyclical internal and effective stresses. Mater Sci Eng. 1984;64(1):L7–L11. doi: 10.1016/0025-5416(84)90083-1

Google Scholar

30. Fournier B, Sauzay M, Caes C, Mottot M, Noblecourt A, Pineau A. Analysis of the hysteresis loops of a martensitic steel - Part II: study of the influence of creep and stress relaxation holding times on cyclic behaviour. Mater Sci Eng A. 2006;437:197–211. doi: 10.1016/j.msea.2006.08.087

Web of Science ® | Google Scholar

31. Fournier B, Sauzay M, Caes C, Noblecourt M, Mottot M. Analysis of the hysteresis loops of a martensitic steel - Part I: study of the influence of strain amplitude and temperature under pure fatigue loadings using an enhanced stress partitioning method. Mater Sci Eng A. 2006;437:183–196. doi: 10.1016/j.msea.2006.08.086

Web of Science ® | Google Scholar

32. Kuhlmann-Wilsdorf D, Laird C. Dislocation behavior in fatigue II. Friction stress and back s ... g.
1979;

33. Cottre ... ess; 1953.

Googl

34. De ... ture, in
plastic
1986;

35. Risbet ... ged
gamm ... que IV.
2001;11(PR4):293–301. doi: 10.1051/jp4:2001436

Google Scholar

36. Guillemer-Neel C, Feaugas X, Clavel M. Mechanical behavior and damage kinetics in nodular cast iron: part II. Hardening and damage. Metall Mater Trans A. 2000;31(12):3075–3085. doi: 10.1007/s11661-000-0086-2

Web of Science ® | Google Scholar

37. Morrison DJ, Jia Y, Moosbrugger JC. Cyclic plasticity of nickel at low plastic strain amplitude: hysteresis loop shape analysis. Mater Sci Eng A. 2001;314(1):24–30. doi: 10.1016/S0921-5093(00)01914-6

Web of Science ® | Google Scholar